

## Lagrangian structures in time-periodic vortical flows

S. V. Kostrykin<sup>1</sup>, A. A. Khapaev<sup>2</sup>, V. M. Ponomarev<sup>2</sup>, and I. G. Yakushkin<sup>2</sup>

<sup>1</sup>Institute of Numerical Mathematics, Russian Academy of Sciences, Moscow, Russia

<sup>2</sup>A.M. Obukhov Institute of Atmospheric Physics, Russian Academy of Sciences, Moscow, Russia

Received: 21 February 2006 – Revised: 6 July 2006 – Accepted: 7 November 2006 – Published: 14 November 2006

**Abstract.** The Lagrangian trajectories of fluid particles are experimentally studied in an oscillating four-vortex velocity field. The oscillations occur due to a loss of stability of a steady flow and result in a regular reclosure of streamlines between the vortices of the same sign. The Eulerian velocity field is visualized by tracer displacements over a short time period. The obtained data on tracer motions during a number of oscillation periods show that the Lagrangian trajectories form quasi-regular structures. The destruction of these structures is determined by two characteristic time scales: the tracers are redistributed sufficiently fast between the vortices of the same sign and much more slowly transported into the vortices of opposite sign. The observed behavior of the Lagrangian trajectories is quantitatively reproduced in a new numerical experiment with two-dimensional model of the velocity field with a small number of spatial harmonics. A qualitative interpretation of phenomena observed on the basis of the theory of adiabatic chaos in the Hamiltonian systems is given.

The Lagrangian trajectories are numerically simulated under varying flow parameters. It is shown that the spatial-temporal characteristics of the Lagrangian structures depend on the properties of temporal change in the streamlines topology and on the adiabatic parameter corresponding to the flow. The condition for the occurrence of traps (the regions where the Lagrangian particles reside for a long time) is obtained.

### 1 Introduction

The study of the Lagrangian trajectory properties in an unsteady incompressible flows is currently one of the problems in hydrodynamics. This problem has numerous applications, including passive tracers transport in the atmosphere and in the ocean. The variety of observed periodic, quasi-periodic and turbulent flows generates different Lagrangian coherent structures that essentially affect transport properties and for example, result in the anomalous transport regimes appear-

ance (Monin and Yaglom, 1971; Ngan and Shepherd, 1999; Linden et al., 2001; Majda and Kramer, 1999).

The description of a Lagrangian particle behavior is based on the equation of fluid-particle motion in the velocity field, which can be specified either in the Eulerian form or in the Lagrangian one (Monin and Yaglom, 1971):

$$\frac{d\mathbf{r}}{dt} = \mathbf{v}_e(\mathbf{r}, t) = \mathbf{u}_l(\mathbf{r}, \mathbf{r}_0, t, t_0) \quad (1)$$

If the Lagrangian field characteristics are specified, it is convenient to describe the tracer transport in terms of particle displacements dispersion and the diffusion coefficient. These characteristics are expressed through the correlation tensor of the Lagrangian velocity, which is obtained by averaging over an ensemble of trajectories (Monin and Yaglom, 1971).

The diffusion coefficient yields a fairly complete description of transport only for the normal diffusion regime, i.e., for the scales on which spatial-temporal correlations of the Lagrangian velocities are not significant. An anomalous diffusion occurs on the scales where these correlations are significant and for which the particle displacements fields usually have a non-Gaussian statistics. A more complete description of the transport process can be obtained by calculating the probability density functions of the displacements for one or two Lagrangian particles in certain points. Such calculations are usually based on the Markovian models of particle random walks that are described by the probabilities of transition between these points or, which is more realistic for complicated flows, between subregions. A model of space-time random walks, i.e., of jumps over random distances occurring at random times, turns out to be more suitable to describe the anomalous regimes associated with the existence of long correlations in the Lagrangian velocity fields. This model leads to an equation of the Montroll-Weiss type, which is applicable for the description of coherent structures (Jones, 1995; Chukbar, 1995).

The problem becomes considerably more complicated if the Eulerian velocity field is known and the Lagrangian field characteristics must be determined. In this case a steady Eulerian field corresponds to particle motions in steady orbits, whereas a temporally periodic Eulerian field results in the space-time randomization of particle trajectories. The case

Correspondence to: S. V. Kostrykin  
(kostr@inm.ras.ru)

of rapidly varying Eulerian velocity fields is studied in sufficient details (Klyatskin, 2001). The study of other cases requires a combination of analytic, numerical and experimental techniques.

The dynamics of Lagrangian particles in two-dimensional divergent-free flows proves to be most accessible for the analysis. The system of equations for the particle motion in the corresponding velocity field is a Hamiltonian system that makes possible application of the known methods for its analysis (Lichtenberg and Lieberman, 1983). One of the directions in recent investigations is the study of flows with a small unsteady periodic component based on Melnikov's works and the Kolmogorov-Arnold-Moser (KAM) theory (Rom-Kedar et al., 1990; Cencini et al., 1999). Another direction is the experimental and numerical study of two-dimensional turbulent flows (Cardoso et al., 1996; Elhmaidi et al., 1993; Haller, 2001). As it is shown in a number of works, the transport in such flows does not lead immediately to a uniform distribution of tracer but it is accompanied by the formation of typical coherent structures.

The study of two-dimensional flows with the time-periodic and steady components of comparable amplitudes is also of a great interest. For such flows the relationship between the Eulerian velocity and the Lagrangian one and a random or regular behavior of Lagrangian trajectories is the main unresolved problem. A laboratory study of these items is particularly important because the theoretical analysis is usually too complicated and requires a number of simplifying assumptions. An experiment with transport in time-dependent Rayleigh-Benard cells is described in Solomon and Gollub (1988); Solomon et al. (1998). More complicated quasi-two-dimensional time-periodic four-vortical flow is experimentally studied in Danilov et al. (1999, 2000) where it is shown that the randomization of the Lagrangian trajectories leads to a rapid transport of tracer inside the regions with the same direction of fluid rotation and a rather slow transport in the region with the opposite direction of fluid rotation. The treatment of such processes can be obtained on the basis of the adiabatic chaos theory (Neishtadt et al., 1991; Veinshtein et al., 1996; Itin et al., 2002)

This paper is devoted to further studying of the Lagrangian trajectories and anomalous transport in quasi-two-dimensional time-periodic flow following Danilov et al. (1999, 2000) and Kostrykin and Yakushkin (2003). The main result of our study consists in reaching a quantitative agreement between measurements and calculations of the admixture transport characteristics. Such an agreement is attained due to a new experimental setup and a model of velocity field reconstruction with correct topological properties. This provides us with a basis for understanding what kind of the Eulerian velocity model can be applied in order to explain the observed transport phenomena. In the paper, we also sum up and develop some results of the preceding studies. In particular, we describe and analyze the generation of Lagrangian coherent structures and determine their life times.

The paper is organized as follows. Some results related to the appearance of structures and chaos in Hamiltonian hydrodynamic systems are considered in Sect. 2. In Sect. 3, the laboratory experiment and the method of numerical modeling are described. Section 4 deals with the comparison of experimental and numerical results. Section 5 discusses the dependence of the Lagrangian coherent structure characteristics on flow parameters. The obtained results are summarized in the Conclusions.

## 2 Structures and chaos in Hamiltonian hydrodynamic systems

In a two-dimensional divergent-free flow, the Eulerian velocity field can be expressed in terms of the streamfunction  $\psi = \psi(\mathbf{r}, t)$

$$\begin{aligned} V_x &= -\frac{\partial\psi}{\partial y}, \\ V_y &= \frac{\partial\psi}{\partial x}. \end{aligned} \quad (2)$$

The streamfunction plays the role of the Hamiltonian and specifies the streamlines topology. It depends parametrically on time. At a given time, two invariants can be calculated at each point:

$$\omega = \Delta\psi, \quad K = \psi_{xx}\psi_{yy} - \psi_{xy}^2. \quad (3)$$

The sign of the vorticity  $\omega$  indicates the direction of vortex rotation, and the sign of the quantity  $K$  corresponds to a different behavior of neighboring trajectories (Okubo-Weiss criterion; Elhmaidi et al., 1993). In other words, the regions with  $K > 0$  and  $K < 0$  are the regions of elliptic and hyperbolic motions, respectively. The fixed points, whose positions are determined by the equation  $\text{grad } \psi(\mathbf{r}_0, t) = 0$ , are also classified. Note that at a fixed point, the quantity  $K$  coincides with the Gaussian curvature of streamfunction at this point. The "instantaneous" separatrices passing through the hyperbolic fixed points are described by the equation  $\psi(\mathbf{r}, t) = \psi(\mathbf{r}_0, t)$  and separate the regions with different character of motion.

In the unsteady flow, the spatial positions of the instantaneous separatrices vary over time. As a consequence, a "separatrix region" arises. From the Eulerian velocity field, one can calculate the areas bounded by the instantaneous separatrices  $I_s(t)$  and the quantity  $K(t)$  for the hyperbolic fixed points and elliptic ones. Using these calculations, one can define the dimensionless quantities  $\alpha = \Delta I_s / I$  (the relative variation of the area bounded by the separatrices) and  $\beta = \langle |K| \rangle^{1/2} / \Omega$ , where  $\langle \cdot \rangle$  is the time-averaged quantity at fixed point and  $\Omega = 2\pi / T$  is the frequency of flow oscillation. The quantity  $\beta$  can be treated as the flow adiabaticity coefficient near a fixed point.

It follows that the transport regimes can be classified according to the methods of their description: transport by rapidly varying velocity fields (e.g., wave ones) with  $\beta \ll 1$ ,

resonance transport by fields with a small unsteady component with  $\alpha \ll 1$  and  $\beta \approx 1$ , and adiabatic transport by quasi-stationary fields with  $\beta \gg 1$ .

For analysis of the Hamiltonian systems, it is convenient to use the action-phase coordinates:  $(I(\psi, t), \phi)$  (Lichtenberg and Lieberman, 1983). The value of the action, which is equal to the area bounded by a streamline at a given  $t$ , remains almost unchanged for a Lagrangian particle, provided that the streamfunction varies sufficiently slowly. If the streamfunction is expressed through the action, as  $\psi = \psi(I, t)$ , the quantity  $\partial\psi/\partial I \sim |K|^{1/2}$  may be treated in the elliptic region as an angular velocity of particle motion along its orbit. In the hyperbolic region, a similar quantity characterizes the relative rate of streamlines divergence (Danilov et al., 2000).

In the case of a steady flow, the particle motion equations in the action-phase coordinates take the form  $I = I_0$ ,  $\phi = \phi_0 + a(I)t$ . It follows that the tracer initial distribution  $F_0(I, \phi)$  transforms with time into a spiral (or a set of spirals). In the case of a random spread of the initial values on the action coordinate, the randomization of particle positions in phase occurs.

For a steady flow disturbed by a time-periodic component, as it follows from the KAM theory, the stable invariant trajectories are conserved in the regions of elliptic motion, and these trajectories break down near the orbits to be resonant with respect to the period of disturbance. At the same time, homoclinic structures appear near the hyperbolic fixed points, which results in randomization of the particle trajectories. The randomization region grows with an increase in the amplitude of the unsteady velocity component (Rom-Kedar et al., 1990; Lichtenberg and Lieberman, 1983).

### 3 Laboratory experiment and numerical simulation method

The laboratory experiment is conducted on the setup described in Danilov et al. (1999, 2000). The setup represents a horizontal tank with dimensions of  $24 \times 12 \text{ cm}^2$  and a depth of 0.7 cm filled with the electrolyte. A four-vortex quasi-two-dimensional flow is generated magneto-hydrodynamically. The amplitude of the velocity field in the vortices is determined by the magnitude of electric current passing through the electrodes. At the critical value of exciting current ( $J = 215 \text{ mA}$ ), the flow becomes unstable and self-oscillating. The oscillations are manifested in the periodic reclosure of the vortices along each of the rectangle diagonals. The measurements are carried out for the electrical current value  $J = 450 \text{ mA}$ , with an amplitude of velocity of the order of a few centimeters per second and oscillation period  $T \approx 50 \text{ s}$ .

The Eulerian velocity field at the surface of fluid, which could be approximated as two-dimensional, is experimentally measured using PIV method. An aluminum powder is used as a passive tracer to study the flow field in the labora-

tory experiment. Because of their small size and mass, the powder clusters may be treated as fluid particles. We use a system of digital analysis of video images to obtain the information on the spatial distribution of tracer particles (Danilov et al., 2000). The analysis of the measurements performed reveals that the two-dimensional velocity field can be treated as approximately divergent-free and consequently the particles motion is governed by some streamfunction. The chosen number of tracks is sufficiently large to reconstruct the streamfunctions at a uniform grid with  $80 \times 44$  mesh points.

Figure 1 shows the topology of instantaneous streamfunctions and the separatrices during a half-period of oscillation. Initially, there are four vortices separated by the separatrix passing through the central hyperbolic fixed point. Further, this separatrix is divided into two branches, one of which (external) continues to separate the flow into the regions with opposite rotations. The second (internal) separatrix separates the merged vortex from smaller vortices. Further the internal separatrix disappears due to the confluence of elliptic fixed points in the corner vortices. During the second half-period, a similar evolution of the vortices occurs, but they are located along the other diagonal.

We subsequently use an expansion of the experimental streamfunction in terms of spatial Fourier harmonics with the time-dependent coefficients:

$$\psi(x, y, t) = \sum a_{kl}(t) \sin\left(\frac{k\pi x}{L_x}\right) \sin\left(\frac{l\pi y}{L_y}\right). \quad (4)$$

One should note that, in Eq. (4), only harmonics satisfying the boundary non-leakage condition are retained. Moreover, because the small-scale harmonics are determined with a relatively large error only the large-scale ones are used in the calculations. We choose the following criteria to find a suitable spectral truncation. First, all harmonics are sorted by the amplitudes, and, for a given number of largest harmonics  $N$ , one can define the truncated streamfunction. Next, we study the behavior of the Gaussian curvature  $K_c(t)$  at the central point  $-(\frac{1}{2}L_x, \frac{1}{2}L_y)$ , which is approximately happened to be fixed in our case. In fact it is exactly fixed only for the central symmetry, but in our case the flow has a weak asymmetry due to the magnetic field distribution. We calculate the  $K_c$  for every spectral truncation starting from  $N=2$  and look for the minimal number of harmonics for which  $K_c(t)$  changes its sign four times during the period of oscillation. In this case, one should expect to obtain the streamfunction topology which will be analogous to that one described above. This criterion is satisfied when the combination of 7 harmonics in space and 3 harmonics in time is chosen. Figure 2 shows the dependence of  $K_c(t)$  for central fixed point and gives us a possibility to estimate the flow adiabaticity coefficient as  $\beta \approx 4.4$ .

One can define an action at some point with a positive value of the streamfunction as the total area enclosed by the streamlines with a given value of  $\psi$ . For the points with

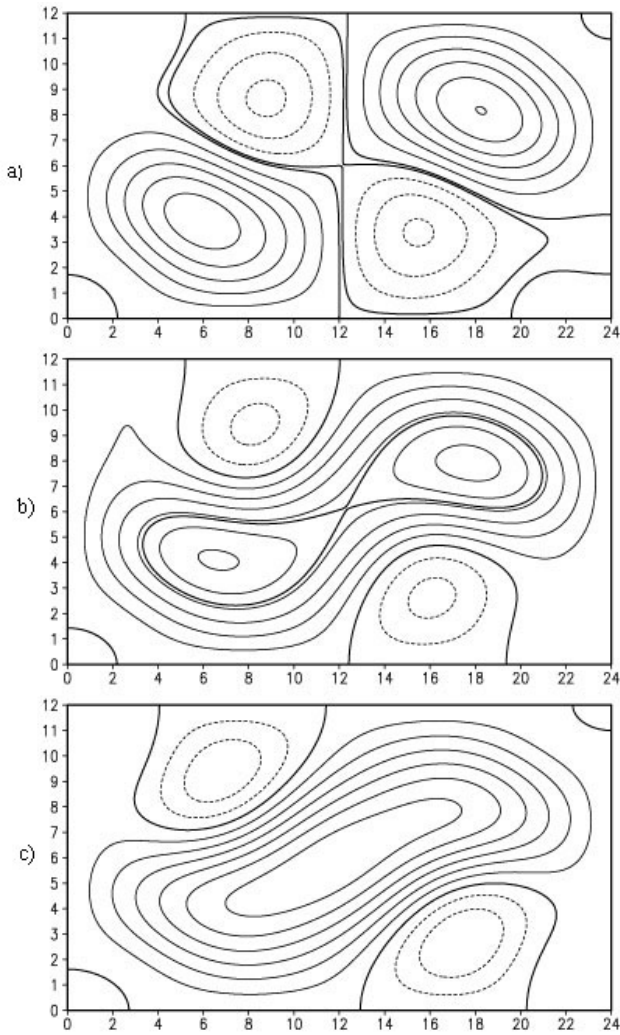


**Fig. 1.** Streamfunction corresponding to  $J=450$  mA at different moments of time during the half period of the flow (thick lines define separatrices: from top **(a)** four vortices when internal and external separatrices are nearly coincided, **(b)** four vortices when internal and external separatrices are different, **(c)** three vortices with elliptic central point.

a negative value of  $\psi$ , we define an action as the difference between the total area occupied by the flow and the area enclosed within the corresponding streamlines. Figure 3 presents the positions of external and internal separatrices in the action-time plane. In a general case, the entire region of action can be divided into three subregions: subregion 1, where equiaction contours do not intersect separatrices (not realized in our case), subregion 2, where equiaction contours intersect the internal separatrix, and subregion 3, where equiaction contours intersect both separatrices.

The Runge-Kutta scheme of the fourth order is used for the numerical calculation of the Lagrangian particles trajectories. We integrate the trajectories of 10 000 particles for

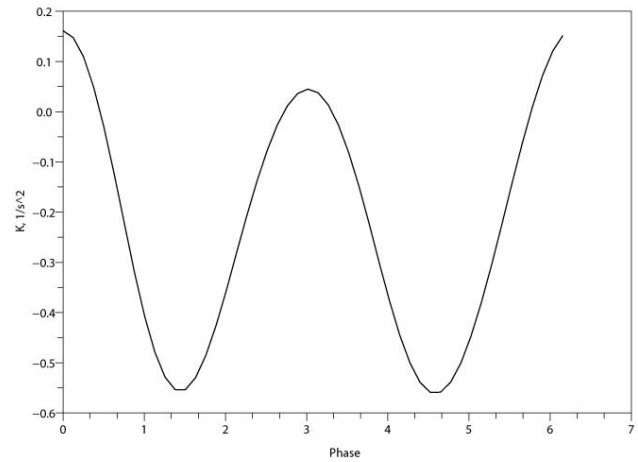


**Fig. 2.** Time-dependence of the Gaussian curvature at the central point.

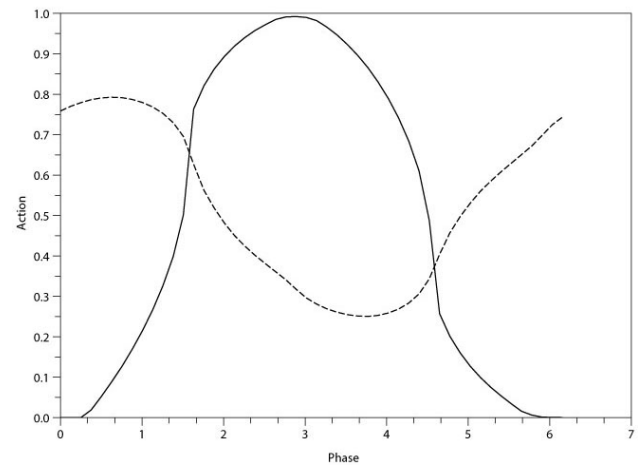


**Fig. 3.** Time-dependence of the action on the external and internal separatrices: solid line is internal separatrix, dashed line is external separatrix.

a time period of  $40T$ . The ensemble-averaged characteristics happen to be insensitive to the doubling of the number of particles and changing of the time step ( $\sim 1$  s) used in the integration.

#### 4 Results of the laboratory and numerical experiments

There are two ways to compare the results of the laboratory and numerical experiments. One can compare the tracer distributions at different moments of time initializing the tracer in one of the corner vortices. The other way is to compare the time evolution of the total number of particles in prescribed regions, for example, in four equal rectangles into which the entire domain is divided at the central point.

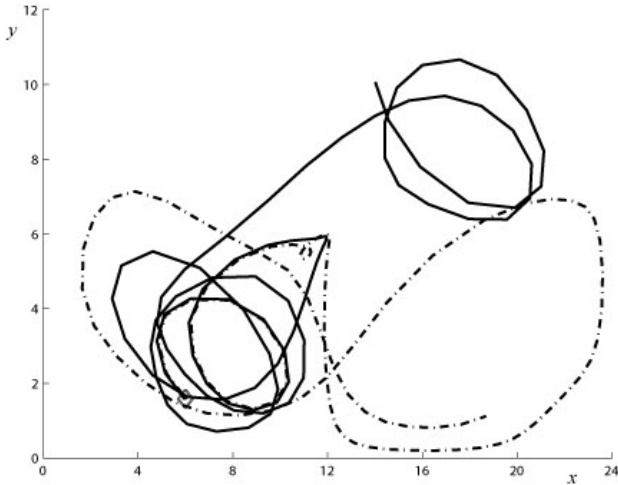


**Fig. 4.** Typical trajectories of the particles during two period of oscillation in the numerical experiment with reconstructed streamfunction (the area of initial particle positions is marked by a diamond).

First, we consider the evolution of tracer patch during one oscillation period. Both data sets show that during the first stage of existence of corner vortices the tracer patch rotates in one of the vortices to form the spiral structure. At the second stage, during which the corner vortices are merged, this structure is elongated and partially transported to the opposite corner. At the last stage, when the central hyperbolic point is formed, the tracer distribution is divided into two main parts. These parts then remain captured in the diagonal corner vortices until the end of the period of oscillation. One should note that the small number of particles may escape from the co-rotating system of vortices and jump to the counter-rotating vortex. The typical trajectories of two particles during first two period of the flow oscillation are presented in Fig. 4. Initially particles are located very close together in the area marked by diamond. But after some time one of them remains in the co-rotating system of vortices while the other one jumps to the counter-rotating vortex. It is interesting to observe that this jump happens near the central hyperbolic point.

Now compare the particle distributions at the moments of time  $t_n = nT$ , where  $n$  is an integer number. Figure 5 shows the evolution of the spatial distribution of tracer over three oscillation periods. One can see that to a large extent, only the vortices located along the same diagonal (with the same direction of rotation) exchange particles. Over several periods, we observe the mixing between these vortices, whereas relatively small number of particles penetrate into the vortices with the opposite circulation. As a result, one can observe the formation of the elongated (phase-extended) structures that exist for several periods. Over time an increasing number of particles leave the vortices to form a chaotic cloud covering the near-separatrix layer and penetrating into the

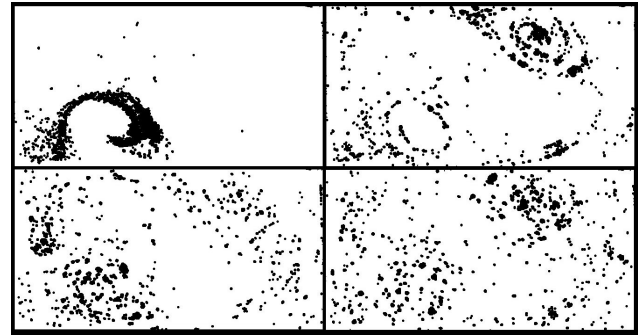


**Fig. 5.** Particles distribution in the laboratory experiment at the different moments of time (from top and left): (a)  $t=0$ , (b)  $t=T$ , (c)  $t=2T$ , (d)  $t=3T$ .

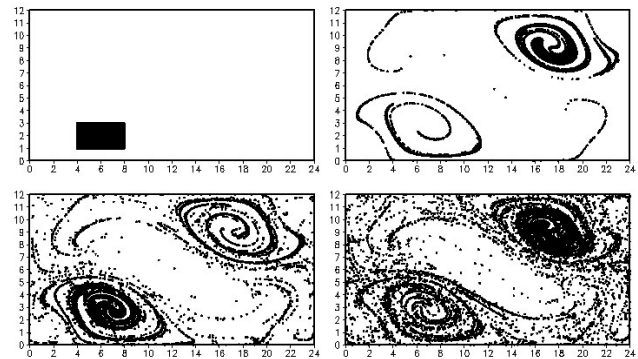


**Fig. 6.** Particles distribution in the numerical experiment with reconstructed streamfunction at the different moments of time (from top and left): (a)  $t=0$ , (b)  $t=T$ , (c)  $t=2T$ , (d)  $t=3T$ .

vortex with opposite circulation. Figure 6 gives the results of the analogous numerical simulation.

Figure 7 shows the relative numbers of particles in four different rectangles that were obtained from both experimental and numerical data. The area inside every rectangle roughly coincides with the area inside the corresponding corner vortex. One can estimate adjustment times in phase (mixing time between the vortices of the same sign) and in action (mixing time between the vortices of the opposite sign) using these results. For example, for the rectangle that encloses all particles at the initial time  $t=0$ , it can be approximated by the formula:

$$g(t) = \frac{3}{8} \left[ \cos\left(\pi \frac{t}{T}\right) \exp\left(-\frac{t}{T_f}\right) + \exp\left(-\frac{t}{T_a}\right) \right] + \frac{1}{4}, \quad (5)$$

where  $T_f$  and  $T_a$  are the adjustment times in phase and in action, respectively. Applying this approach to the numerical data, we get the following estimates for the adjustment times:  $T_a = 10.1T$  and  $T_f = 3.4T$ . Since  $T_f \ll T_a$  it follows that during period of time  $t < T_f$  the particle exchange between co-rotating vortices is strong and between counter-rotating vortices is relatively weak.

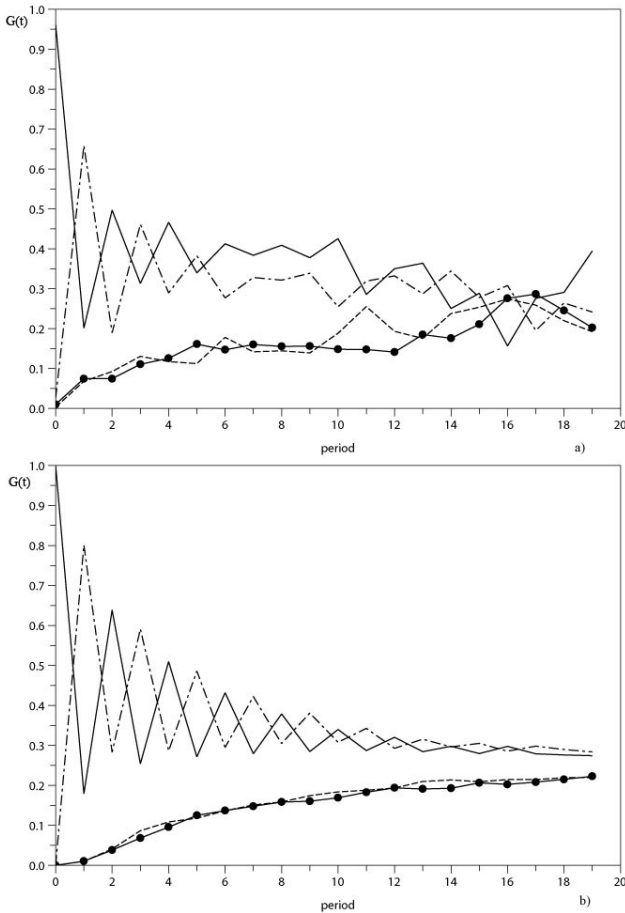


**Fig. 7.** Time-dependence of relative number of particles inside four equal rectangles: **(a)** laboratory experiment, **(b)** numerical experiment. Solid line is low left rectangle, dashed line is upper left rectangle, short-dashed dotted line is upper right rectangle, black circles is low right rectangle.

The measurement data on tracer transport are well interpreted on the basis of concept of the adiabatic regime (Danilov et al., 1999, 2000). In the adiabatic limit the action is an invariant. A “rapid” mechanism associated with the motion along the lines of constant action is responsible for tracer redistribution between the vortices with the same direction of rotation, because their merging and breaking are not accompanied by a change in the total action. Actually, the motion is close to the ideally adiabatic motion until one of the particles intersects a separatrix. When the separatrix is intersected, i.e., at the times  $t_s$  where  $I=I_s(t_s)$ , the action changes by  $\Delta I \sim 1/\beta$ . More precisely, both the violation of adiabaticity and a noticeable change in the action occur when the particles travel through the region of hyperbolic motion adjacent to the separatrix. A “slow” mechanism, which is associated with a change in action, arises due to the intersection of the separatrix by a particle and leads to the transport of particles into the vortices of opposite direction of rotation.

## 5 Structural properties of Lagrangian trajectories and tracer transport in two-parametrical flow

Another interesting possibility is to study the dependence of a passive scalar transport on the flow parameters. For this purpose we use a simplified streamfunction with a topological structure similar to the streamfunction obtained from the measurements (Danilov et al., 2000). This simple two-parametric streamfunction is not appropriate for a quantitative explanation of experimental data, but it is convenient for a qualitative analysis:

$$\begin{aligned} \psi(\mathbf{r}, t) &= B [\psi_0(\mathbf{r}) + A\psi_1(\mathbf{r}, t)], \\ \psi_0 &= C_{22} \sin\left(\frac{2\pi x}{L_x}\right) \sin\left(\frac{2\pi y}{L_y}\right) \\ &\quad + C_{42} \sin\left(\frac{4\pi x}{L_x}\right) \sin\left(\frac{2\pi y}{L_y}\right), \\ \psi_1 &= \left[ C_{11} \sin\left(\frac{\pi x}{L_x}\right) \sin\left(\frac{\pi y}{L_y}\right) \right. \\ &\quad \left. + C_{13} \sin\left(\frac{\pi x}{L_x}\right) \sin\left(\frac{3\pi y}{L_y}\right) \right] \sin(\Omega t) - \\ &\quad - C_{31} \sin\left(\frac{3\pi x}{L_x}\right) \sin\left(\frac{\pi y}{L_y}\right) \cos(\Omega t), \end{aligned} \quad (6)$$

where  $L_x$  and  $L_y$  are the dimensions of the cell,  $\Omega=2\pi/T$ ,  $C_{22}=3.1 \text{ cm}^2/\text{s}$ ,  $C_{42}=1.1 \text{ cm}^2/\text{s}$ ,  $C_{11}=4.1 \text{ cm}^2/\text{s}$ ,  $C_{31}=2.8 \text{ cm}^2/\text{s}$ ,  $C_{13}=1.2 \text{ cm}^2/\text{s}$ ,  $T=50 \text{ s}$ . This flow field depends on two parameters:  $A$  (the relative amplitude of the non-stationary part of the flow) and  $B$  (the scale factor of the flow amplitude). It is possible to show that the parameter  $A$  characterizes relative variations of the area bounded by separatrices ( $\alpha$ ) and with an increase in  $A$  the value  $\alpha$  also increases. The parameter  $B$  is similar to the adiabaticity parameter ( $\beta$ ).

Spatial structures arising in the distribution of tracer are described by the Poincaré sections for  $t_n=t_0+nT$ . As a reference phase we chose  $t_0=0$  when there are two isolated vortices along one diagonal (right-hand rotation) and one merged vortex along the other diagonal. This topology is maintained for a larger part of a half-period of oscillation. The model results for the tracer patch initially located in the low right corner are shown in Figs. 8–10, where the Poincaré sections are given for a different number of periods ( $n=1, 2, 4, 8$ ).

As it can be seen from Fig. 8, if  $A=1$  and  $B=1$ , the particle distribution forms helical structures similar to the case with reconstructed streamfunction (4). After one period a portion of tracer transfers into the other vortex with the same direction of rotation, changing the action value only slightly. Additionally, when a separatrix is intersected, an extended “tail” is formed inside the central vortex. After one oscillation period the tracer is redistributed between the vortices, holding a helical structure in each of the vortices. The structures belonging to the central vortex are formed from the

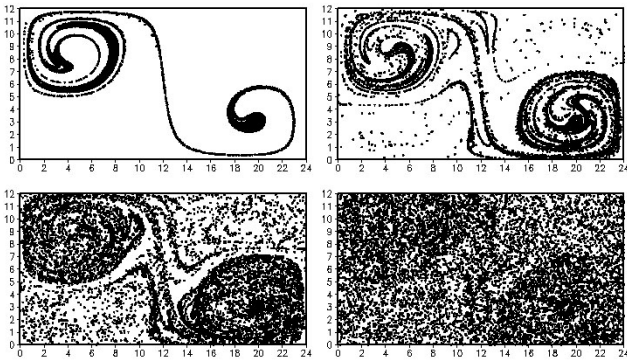


**Fig. 8.** Particles distribution in the numerical experiment with two-parametrical streamfunction ( $A=1$ ,  $B=1$ ) at the different moments of time (from top and left): (a)  $t=T$ , (b)  $t=2T$ , (c)  $t=4T$ , (d)  $t=8T$ .

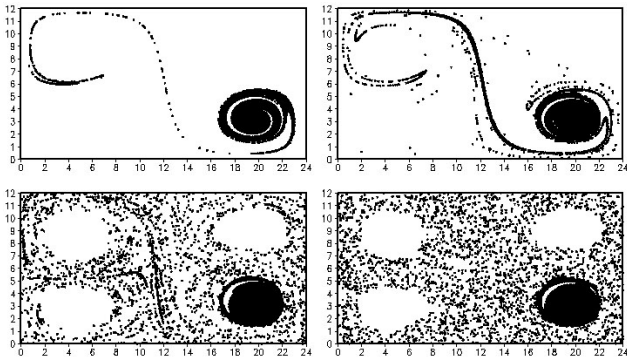


**Fig. 9.** The same as in Fig. 8, but for  $A=0.5$ ,  $B=1$ .

“tails” appearing every period. Thus, a Lagrangian trajectory can be represented as a set of quasi-regular segments of an ideally adiabatic motion. Appearance of a few segments is connected with the particles jump to another orbits, which occurs when separatrix intersects the Lagrangian trajectories. Particle walks happen between the regions of partially stable motions adjacent to the elliptic points. These characteristic tracer structures are formed during a few periods. After eight periods of oscillation they begin to destroy and the particle segments uniformly occupy the entire region of the flow.

Figures 9 and 10 demonstrate the structure formation in the cases of  $A=0.5$ ,  $B=1$  and  $A=1$ ,  $B=4$ , respectively. As one can see, in these cases an increase in the adiabaticity parameter  $B$  leads to the slowing down of the transport into the vortices with opposite directions of rotation and, consequently, to the smoothing of tracer concentration. To estimate this effect quantitatively we calculate an adjustment time in action using the Eq. (5). The dependence of  $T_a$  on the parameter  $B$  is presented in Fig. 11. One should note that in all experiments with this two-parametrical flow we had  $T_f < T$ . This is due to the roughness of the 5-harmonics model. In the more complex model with 21 harmonics  $T_f$  is much closer to the observed values (compare Figs. 7a and b).

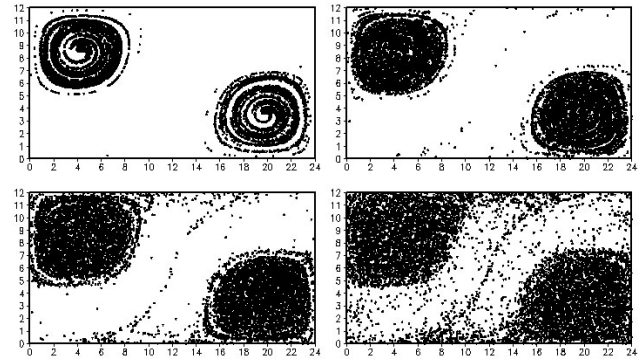


**Fig. 10.** The same as in Fig. 8, but for  $A=1$ ,  $B=4$ .

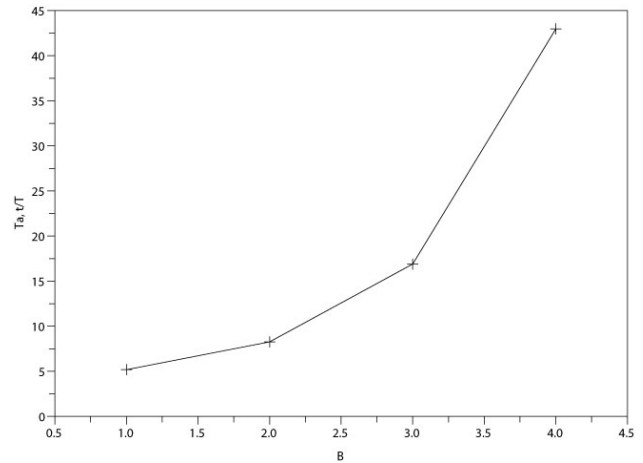


**Fig. 11.** Dependence of the adjustment time in action  $T_a$  on the adiabaticity parameter  $B$ .

As it can be seen from Figs. 8–9, a decrease in  $A$  results in the formation of strongly stagnant zones, which are decoupled or weakly coupled with the remaining flow. In the regions completely untouched by the separatrix displacements the stagnant zones appear. It corresponds to the case when in the action-phase space the regions unreachable by the separatrices exist.

## 6 Conclusions

New laboratory and numerical studies (specifying the performed early in Danilov et al., 2000; Kostrykin and Yakushkin, 2003) of the Lagrangian particle transport in quasi-two-dimensional time periodic flow that can generate chaotic trajectories are conducted. A fast transport of particle into the vortices with a same direction of rotation and a much slower transport into the vortices with the opposite direction of rotation is observed. As it is shown in our previous studies, a fairly slow change in the system velocity field means that such experiments can be interpreted from the point of view

of the adiabatic chaos theory. Previous attempts of numerical simulations using the model approximation of field velocity gave us only a qualitative explanation of the observed picture. In present work we obtain the quantitative agreement between the evolution pattern of tracer distribution and the data of numerical simulation using the measured velocity fields. To achieve this agreement the velocity model must conserve the main features of flow topology and its temporal variation. We suggested here a simple phenomenological model of transport phenomena. This model contains two characteristic times describing a transition of the Lagrangian particles between co-rotating and counter-rotating vortices respectively.

To analyze the adiabaticity factor on the particles transport the simple two-parametrical presentation of velocity field is used. The simulations performed demonstrate that characteristic transport times increase when adiabaticity coefficient grows. The obtained numerical results allow us to suggest that the transport between vortices depends on local flow properties near fixed points. The Lagrangian transport includes three major stages: transport along equiaction contours, transport in action, and mixing of the tracer concentration in the entire region. Lagrangian trajectories of liquid particles combine features of regularity and randomness, in particular, the coherent structures with certain lifetime are generated. The results of the numerical simulation indicate that with an increase of the flow adiabaticity coefficient the Lagrangian trajectories stay near equiaction contours over increasingly longer periods of time. Moreover, a change in the separatrix region size can result to the formation of stagnant zones or “traps”.

For fairly high values of the adiabaticity coefficient a more complete description of the diffusion process in the action space can be obtained by using a generalized model of particle random walks in the action-time space. For such generalized model additional elaborations are necessary. The further investigation of this problem can also involve both two-particles dispersion and coherent structures relation to finite-time Lyapunov exponents.

It is necessary to note that the conclusions following from the simulation performed in this work may prove to be valid for studying the tracer transport by different quasi-two-dimensional atmospheric flows including two-dimensional turbulence.

*Acknowledgements.* This work is supported by Russian Foundation for Basic Research (projects Nos. 04-05-64044, 05-05-64745) and by the grant of the President of Russian Federation MK-532.2006.5.

We dedicate this work to memory of S. S. Moiseev.

Edited by: N. S. Erokhin

Reviewed by: A. Neishtadt and two other referees

## References

- Cardoso, O., Gluckmann, B., Parcollet, O., and Tabeling, P.: Dispersion in a quasi-two-dimensional turbulent flow: an experimental study, *Phys. Fluids A*, 8, 209–214, 1996.
- Cencini, M., Lacorata, G., Vulpani, A., and Zambianchi, E.: Mixing in a meandering jet: a Markovian approximation, *J. Phys. Oceanog.*, 29, 2578–2594, 1999.
- Chukbar, K. V.: Stochastic transport and fractional derivatives, *J. Exp. Theor. Phys.*, 81, 1025–1029, 1995.
- Danilov, S. D., Dovzhenko, V. A., Karpilova, O. I., and Yakushkin, I. G.: Passive tracer transport in a nonstationary four-vortex hydrodynamic system, *Izv., Atmos. Ocean. Phys.*, 35, 733–743, 1999.
- Danilov, S. D., Dovzhenko, V. A., and Yakushkin, I. G.: Transport of a passive scalar and Lagrangian chaos in a Hamiltonian hydrodynamic system, *J. Exp. Theor. Phys.*, 91, 423–432, 2000.
- Elhmaidi, D., Provinzale, A., and Babiano, A.: Elementary topology of two-dimensional turbulence from a Lagrangian viewpoint and single-particle dispersion, *J. Fluid Mech.*, 257, 533–558, 1993.
- Itin, A. P., de la Llave, R., Neishtadt, A. I., and Vasiliev, A. A.: Transport in a slowly perturbed convective cell flow, *Chaos*, 12, 1043–1053, 2002.
- Jones, S.: Dispersion in zero-mean flow, *Phys. Fluids A*, 7, 898–900, 1995.
- Haller, G.: Lagrangian coherent structures and the rate of strain in two-dimensional turbulence, *Phys. Fluids A*, 13, 3365–3385, 2001.
- Klyatskin, V. I.: *Stochastic equations through the eyes of a physicist*, Amsterdam, Elsevier, 2005.
- Kostrykin, S. V. and Yakushkin, I. G.: Passive tracers transport and Lagrangian structures in unsteady vortical flows, *Izv., Atmos. Ocean. Phys.*, 39, 675–684, 2003.
- Lichtenberg, A. J. and Lieberman, M. A.: *Regular and stochastic motion*, New York: Springer, 1983.
- Linden, P. F. and Redondo, J. M.: *Turbulent mixing in geophysical flows*, Eds., Barcelona, 2001.
- Majda, A. J. and Kramer, P. R.: Simplified models for turbulent diffusion, *Phys. Reports*, 314, 239–572, 1999.
- Monin, A. S. and Yaglom, A. M.: *Statistical fluid mechanics*, Cambridge, Mass.: MIT Press, vol. 1, 1971, vol. 2, 1975.
- Neishtadt, A. I., Chaikovskii, D. K., and Chernikov, A. A.: Adiabatic chaos and diffusion of particles, *J. Exp. Theor. Phys.*, 72, 423–430, 1991.
- Ngan, K. and Shepherd, T. G.: A closer look at chaotic advection in the stratosphere. Part I: geometric structure, *J. Atmos. Sci.*, 56, 4134–4152, 1999.
- Rom-Kedar, V., Leonard, A., and Wiggins, S.: An analytical study of transport, mixing and chaos in an unsteady vortical flow, *J. Fluid Mech.*, 214, 347–394, 1990.
- Solomon, T. H. and Gollub, J. P.: Chaotic particle transport in time-dependent Rayleigh-Benard convection, *Phys. Rev. A*, 38, 6280–6286, 1988.
- Solomon, T. H., Tomas, S., and Warner, J. L.: Chaotic mixing of immiscible impurities in a two-dimensional flow, *Phys. Fluids*, 10, 342–350, 1998.
- Veinshtein, D. L., Vasiliev, A. A., and Neishtadt, A. I.: Adiabatic chaos in a two-dimensional mapping, *Chaos*, 6, 514–518, 1996.